

## Demonstration of a Low Threshold Current in 1.54 $\mu\text{m}$ InAs/InP(311)B Quantum Dot Laser with Reduced Quantum Dot Stacks

Estelle HOMEYER\*, Rozenn PIRON, Frédéric GRILLOT, Olivier DEHAESE, Karine TAVERNIER, Erwan MACÉ, Jacky EVEN, Alain LE CORRE, and Slimane LOUALICHE

FOTON-LENS, UMR CNRS C6082, INSA de Rennes, 20 Avenue des Buttes de Coësmes, CS 14315, F34043 Rennes Cedex, France

(Received May 10, 2007; accepted May 25, 2007; published online October 9, 2007)

This article reports the improvement of broad area lasers epitaxially grown on InP(311)B substrate. Thanks to optimized growth techniques, a high density of uniformly sized InAs quantum dots (QDs) up to  $10^{11} \text{ cm}^{-2}$  is obtained. The device, which contains only two stacks of QDs, exhibits a ground state laser emission at 1.54  $\mu\text{m}$  at room temperature associated with a threshold current density as low as  $170 \text{ A/cm}^2$ . Experimental results also demonstrate a modal gain greater than  $8 \text{ cm}^{-1}$  per QD plane. [DOI: 10.1143/JJAP.46.6903]

KEYWORDS: quantum dots, semiconductor laser, InP substrate

Much research is devoted to the realization of optical semiconductor devices, and especially lasers with quantum dots (QDs) as an active medium.<sup>1)</sup> QDs are structures where the confinement takes place in the three dimensions of space, which leads to very attractive properties, such as low threshold current,<sup>2)</sup> high differential gain,<sup>3)</sup> and low temperature sensitivity.<sup>4)</sup> A lot of effort has been devoted so far to the GaAs-based QD material system for 1.3  $\mu\text{m}$  applications, thanks to a better material maturity.<sup>5)</sup> Careful control of the strain and spacer thickness between adjacent QD layers has allowed the demonstration of relatively high modal gain structures,  $22 \text{ cm}^{-1}$  for eight QD layers.<sup>6)</sup> This value however is still lower than that of a standard quantum well (QW) structure ( $\sim 50\text{--}60 \text{ cm}^{-1}$ ). Recent results also report laser emission at higher wavelengths such as those obtained using InAs metamorphic QDs on GaAs.<sup>7)</sup> Thus 1.45  $\mu\text{m}$  metamorphic lasers with a very low threshold ( $63 \text{ A/cm}^2$ ) as well as a large  $T_0$  (550 K)<sup>8)</sup> have been demonstrated. However, despite all these results, the targeted 1.55  $\mu\text{m}$  wavelength required for long-haul applications remains difficult to obtain.

Instead of GaAs, an alternative consists in using InP substrate which allows an emission at 1.55  $\mu\text{m}$ .<sup>9)</sup> Depending on the substrate orientation and type of epitaxy, different nanostructure shapes are obtained. Growth using molecular beam epitaxy (MBE) leads to the formation of quantum dots on (311)B-oriented InP substrates, while on (100)-oriented substrate, quantum dashes are mostly obtained.<sup>10)</sup> On the other hand, metal organic vapour phase epitaxy (MOVPE) leads to QD structures on (100) InP substrates, usually with a lower QD density.<sup>11)</sup> Recent publications report the achievement of a InGaAs QD density of more than  $10^{11} \text{ cm}^{-2}$ , but lasers made with those nanostructures in the active area show high threshold current densities above  $1 \text{ kA/cm}^2$ .<sup>12)</sup>

One of the main advantages arising from the InP(311)B orientation is that it makes it possible to obtain three-dimensional confined nanostructures with high QD densities which leads to high gain laser structures.<sup>13)</sup> Previous works have already demonstrated encouraging results at room temperature (RT) with this type of structure.<sup>14)</sup> As a consequence, the aim of this article is to present improved performances of InAs/InP(311)B QD broad area lasers. By reducing the number of QD stacks in the active zone, a low threshold current density as well as a high modal gain is

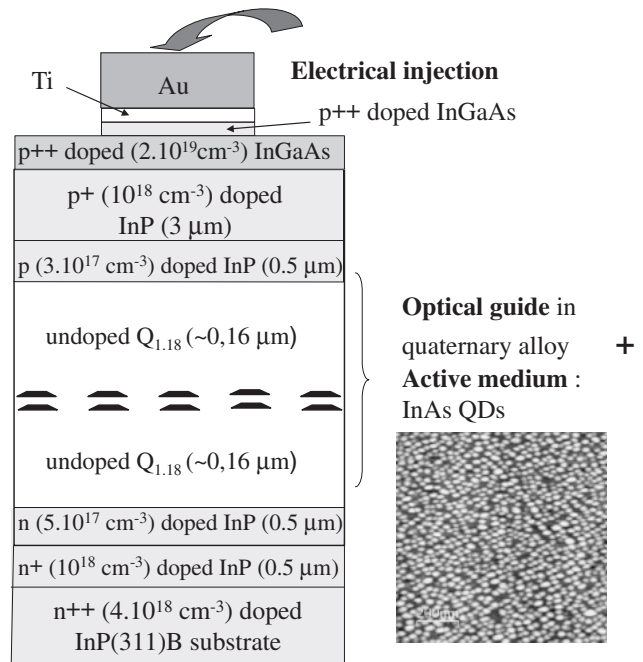


Fig. 1. Schematic drawing of the InAs/InP laser structure, containing two InAs QD layers. A  $1 \mu\text{m}^2$  AFM image is given in insert: average diameter of 30 nm and average height of 5 nm could be deduced. The QD density was evaluated to be higher than  $10^{11} \text{ cm}^{-2}$ .

reported. These state of the art results obtained thanks to several growth optimizations are promising for the next generation telecommunication networks for low cost devices, allowing cooler-free and isolator-free operations.<sup>15)</sup>

The laser structure was grown by gas source MBE on n-type (311)B oriented InP substrate. Figure 1 shows the laser structure, which consists in a wave guide of  $0.16 \mu\text{m}$  of lattice-matched quaternary alloy  $\text{Ga}_{0.2}\text{In}_{0.8}\text{As}_{0.43}\text{P}_{0.57}$  ( $Q_{1.18}$ ) with a gap emission wavelength at 1.18  $\mu\text{m}$  on both sides of the active area. This active area is composed of only two layers (separated by 30 nm of  $Q_{1.18}$ ) of InAs QDs, self assembled using the Stranski–Krastanov mode. Two growth optimizations have been performed on this sample: a reduction of the arsenic flux during the growth,<sup>16)</sup> and the double cap procedure.<sup>17)</sup> The reduction of the arsenic flux during the growth makes it possible to reach a high QD density. This QD density is of first importance so as to realize laser structures with high material gain as well as to

\*E-mail address: Estelle.Homeyer@ens.insa-rennes.fr

ensure an efficient lateral coupling between the dots, which has been shown to improve the laser efficiency for a well selected coupling regime.<sup>18)</sup> The so-called double cap procedure, described in ref. 19 has been used to reduce the size dispersion of the QDs, by controlling their height through the height of the first capping layer. A sharper gain curve can consequently be expected for the structure, which greatly eases the losses compensation. Furthermore, the emission energy of the laser, strongly linked to the QD size, can be controlled by this technique. As a result, the wavelength can be tuned to the required 1.55  $\mu\text{m}$  telecommunication wavelength.

The inset of Fig. 1 is a 1  $\mu\text{m}^2$  atomic force microscopy (AFM) image of uncapped dots grown as described above. This structural analysis has made it possible to determine QD dimensions. A diameter and height of 30 and 5 nm respectively have been deduced as well as a QD density above  $10^{11} \text{ cm}^{-2}$ . However, the height of the first capping layer being set at 3 nm, the final height of covered dots is estimated at a maximum of 3 nm, as confirmed by transmission electron microscopy (TEM) measurements.<sup>19)</sup> The carrier confinement was then studied by magneto-photoluminescence in the QDs, depending on the composition of the first capping layer.<sup>20)</sup> It was demonstrated that using  $Q_{1.18}$  provided better carrier confinement than InP, by preventing the intermixing effect observed in InAs/InP and InAs/GaAs QDs.<sup>21)</sup> Cross-sectional scanning tunneling microscopy (X-STM) measurements have confirmed the homogeneity of the InAs QDs.<sup>22)</sup>

Photoluminescence (PL) measurements were performed on this device at RT under continuous 647 nm wavelength laser excitation. Figure 2 shows a PL peak at 0.79 eV (1.57  $\mu\text{m}$ ), with a full width at half maximum (FWHM) of 49 meV (91 nm). This linewidth, comparable with the best values obtained on this type of substrate,<sup>9)</sup> reveals a low size dispersion of the QDs, attributed both to the use of substrate orientation (311)B and to the double cap procedure. The use of a small number of QD layers also contributes by preventing the increase of the QD size, often observed when many layers are stacked, and leading to higher size dispersion. This is of great importance for the realization of simplified and low cost devices with high performance.

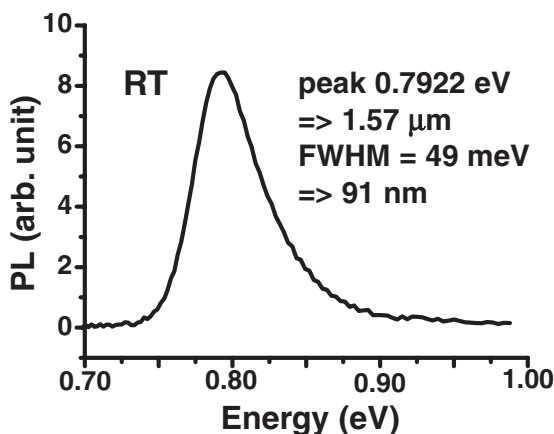


Fig. 2. The PL spectrum shows a peak at 0.79 eV (corresponding to a 1.57  $\mu\text{m}$  wavelength), and a FWHM of 49 meV (91 nm). This low FWHM can be explained by the reduced QD size dispersion due to optimized growth.

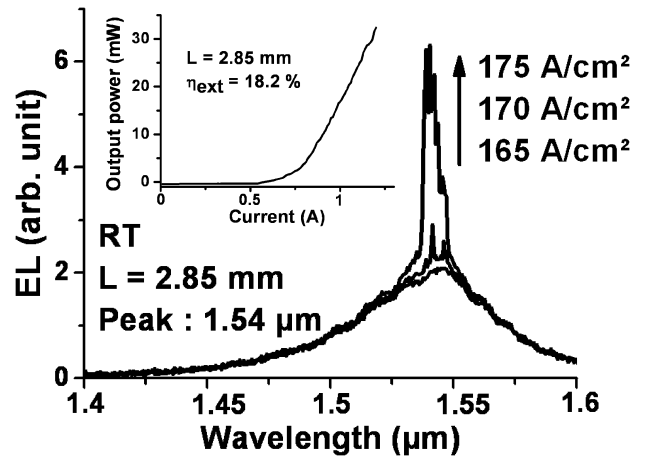


Fig. 3. EL spectra obtained at RT, for the 2.85 mm cavity length. Lasing occurs on the ground state at 1.54  $\mu\text{m}$ , for a threshold current density of 170  $\text{A}/\text{cm}^2$ . As an insert is given the light-current curve for this device. It demonstrates a total external efficiency of 18.2%.

Laser structures were processed. Conventional edge-emitting lasers of various lengths, with 100- $\mu\text{m}$ -wide ridge structures, were obtained by wet chemical etching. The cavities have as cleaved-facets on both ends, which means an approximate reflectivity of 30% on both sides. Electroluminescence (EL) spectra at RT were obtained with pulsed electrical injection (500 ns pulse width, 0.1% duty cycle) on the 2.85 mm long device (cf. Fig. 3). They show a threshold current density as low as 170  $\text{A}/\text{cm}^2$ , which is to our knowledge the best result obtained with this type of structure on InP substrate. This performance is all the more remarkable that the active area contains only two layers of QDs. This point is of first importance for the realization of future ridge waveguide (RWG) since stacking a high number of uniform QD layers increases the waveguide thickness and may disturb the single mode operation. Emission is obtained on the ground state (GS) transition at 1.54  $\mu\text{m}$ , which is in agreement with the peak of the PL spectrum.

Insert in Fig. 3 gives the light current curve for this device. An external efficiency of 73 mW/A per facet is deduced. This corresponds to a total external efficiency of 18.2%. Internal losses on InP have been estimated on average to  $10 \text{ cm}^{-1}$  which matches with values already published in the literature ( $7\text{--}11 \text{ cm}^{-1}$ ).<sup>10,23,24)</sup> An internal efficiency of 62% has been evaluated for this device, which is comparable to values usually obtained on this type of structure.<sup>10)</sup> Power saturation has not been investigated on this device, although it seems to exceed 30 mW.

In Fig. 4, the threshold current density achieved under pulsed excitation at RT is reported as a function of the inverse of cavity length for cavity lengths ranging from 1 to 2.85 mm. For cavities longer than 2 mm, GS lasing occurs at a peak position at 1.54  $\mu\text{m}$  in accordance with the PL measurement. The lasing wavelength starts decreasing from 1.53  $\mu\text{m}$  for a 1.75 mm long cavity, down to 1.495  $\mu\text{m}$  for a 1 mm cavity length. At the same time, the threshold current density at RT increases non linearly, from 170  $\text{A}/\text{cm}^2$  for a 2.85 mm long cavity, up to 750  $\text{A}/\text{cm}^2$  for the 1 mm cavity.

This effect can be explained because structures grown on InP show a great overlap between GS and ES gain curves,<sup>18)</sup>

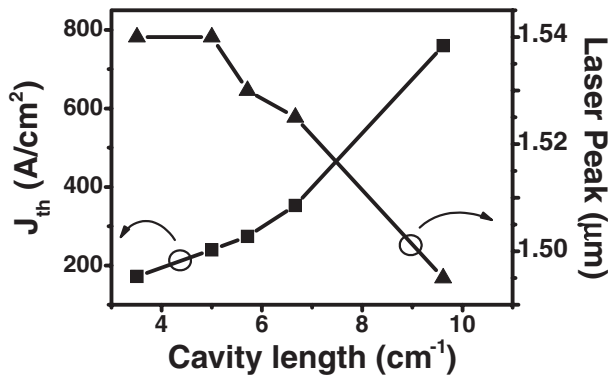


Fig. 4. Threshold and laser peak as a function of the inverse of the cavity length.

as observed by high power photoluminescence experiments. Indeed GS and ES are actually separated by only an average of 25 meV, and their FWHM is larger than 25 meV. Consequently, when losses increase, the first ES level starts to be filled before the GS level is totally saturated. This leads, by carrier redistribution explained in ref. 25, to the progressive change of the lasing wavelength from 1.52 to 1.47 μm, which corresponds to the expected energy difference between GS and ES, of about 25 meV.<sup>26</sup> In the case of InAs/GaAs QDs, where there is no overlap between GS and ES, the lasing wavelength switches abruptly from GS to ES.<sup>27</sup>

The maximum modal gain of the ground state transition is thus difficult to evaluate. The point where the ground state is fully saturated on InP structures cannot be evaluated precisely, but it is clear that it happens here for a cavity shorter than 2 mm. Mirror losses, given by the expression  $\alpha_m = -\ln(R)/L$ , where  $R$  is the facet reflectivity (0.3) and  $L$  the Fabry–Perot cavity length, are equal to  $6\text{ cm}^{-1}$  for a 2 mm cavity length. As said above, internal losses ( $\alpha_i$ ) are taken to a  $10\text{ cm}^{-1}$  value. The modal gain, given by  $g = \alpha_i + \alpha_m$ , of the ground state transition can therefore be estimated to a minimum value of  $8\text{ cm}^{-1}$  per QD plane.

Taking into account that the overlap of the QD plane with the optical mode is estimated to a value of 0.43%, and the QD surface occupancy to a factor of  $\sim 80\%$ , the minimum expected value of the absorption coefficient of the QD plane can be evaluated to  $2300\text{ cm}^{-1}$ . An absorption coefficient of  $4400\text{ cm}^{-1}$  has been directly measured previously on QD structures with  $5 \times 10^{10}\text{ cm}^{-2}$  density.<sup>28</sup> By comparison with this value, the absorption for the structure with a QD density of  $10^{11}\text{ cm}^{-2}$  can thus be estimated close to  $9000\text{ cm}^{-1}$ , which is comparable to the absorption coefficient of InGaAs/InP QW structures.

In summary, a 2.85 mm broad area laser, grown on InP(311)B substrate and with an active zone containing only two layers of InAs QDs, has been realized. A lasing emission centered at 1.54 μm, and a threshold current density as low as  $170\text{ A/cm}^2$  at RT have been demonstrated. It has also been shown that this device presents a modal gain of  $8\text{ cm}^{-1}$  per QD layer for the ground state transition. These results can be explained through the optimization of growth techniques. To the best of our knowledge, those performances obtained with a reduced QD stacks are state of the art for QD lasers grown on InP substrate, and are promising for

the realization of future high frequency modulated laser and optical amplifier working at the 1.55 μm optical telecommunication wavelength.

- 1) D. Bimberg: *J. Phys. D* **38** (2005) 2055.
- 2) G. Park, O. B. Shchekin, D. L. Huffaker, and D. G. Deppe: *IEEE Photonics Technol. Lett.* **12** (2000) 230.
- 3) A. Sahli, L. Martiradonna, G. Visimberga, V. Tasco, L. Fortunato, M. T. Todaro, R. Cingolani, A. Passaseo, and M. De Vittorio: *IEEE Photonics Technol. Lett.* **18** (2006) 1735.
- 4) S. S. Mikhlin, A. R. Kovsh, I. L. Krestnikov, A. V. Kozhukhov, D. A. Livshits, N. N. Ledentsov, Yu. M. Shernyakov, I. I. Novikov, M. V. Maximov, V. M. Ustinov, and Zh. I. Alferov: *Semicond. Sci. Technol.* **20** (2005) 340.
- 5) D. Bimberg, N. Kirstaedter, N. N. Ledentsov, Zh. I. Alferov, P. S. Kop'ev, and V. M. Ustinov: *IEEE J. Sel. Top. Quantum Electron.* **3** (1997) 196.
- 6) J. P. Reithmaier and A. Forchel: *IEEE J. Sel. Top. Quantum Electron.* **8** (2002) 1035.
- 7) I. I. Novikov, N. Yu Gordeev, M. V. Maximov, Yu. M. Shernyakov, A. E. Zhukov, A. P. Vasil'ev, E. S. Semenova, V. M. Ustinov, N. N. Ledentsov, D. Bimberg, N. D. Zakharov, and P. Werner: *Semicond. Sci. Technol.* **20** (2005) 33.
- 8) Z. Mi, P. Bhattacharya, and J. Yang: *Appl. Phys. Lett.* **89** (2006) 153109.
- 9) H. Saito, K. Nishi, and S. Sugou: *Appl. Phys. Lett.* **78** (2001) 267.
- 10) R. H. Wang, A. Stintz, P. M. Varangis, T. C. Newell, H. Li, K. J. Malloy, and L. F. Lester: *IEEE Photonics Technol. Lett.* **13** (2001) 767.
- 11) J. W. Jang, S. H. Pyun, S. H. Lee, I. C. Lee, W. G. Jeong, R. Stevenson, P. Dapkus, N. J. Kim, M. S. Hwang, and D. Lee: *Appl. Phys. Lett.* **85** (2004) 3675.
- 12) N. J. Kim, Y. D. Jang, J. S. Yim, J. H. Lee, D. Lee, S. H. Pyun, W. G. Jeong, and J. W. Jang: *J. Korean Phys. Soc.* **48** (2006) 1210.
- 13) S. Fréchengues, V. Drouot, N. Bertru, B. Lambert, S. Loualiche, and A. Le Corre: *J. Cryst. Growth* **201–202** (1999) 1180.
- 14) P. Caroff, C. Paranthoën, C. Platz, O. Dehaese, H. Folliot, N. Bertru, C. Labbé, R. Piron, E. Homeyer, A. Le Corre, and S. Loualiche: *Appl. Phys. Lett.* **87** (2005) 243107.
- 15) O. Carroll, I. O'Driscoll, S. P. Hegarty, G. Huyet, J. Houlihan, E. A. Viktorov, and P. Mandel: *Opt. Express* **14** (2006) 10831.
- 16) P. Caroff, N. Bertru, A. Le Corre, O. Dehaese, T. Rohel, I. Alghoraibi, H. Folliot, and S. Loualiche: *Jpn. J. Appl. Phys.* **44** (2005) L1069.
- 17) P. Caroff, N. Bertru, C. Platz, O. Dehaese, A. Le Corre, and S. Loualiche: *J. Cryst. Growth* **273** (2005) 357.
- 18) C. Cornet, M. Hayne, P. Caroff, C. Levallois, L. Joulaud, E. Homeyer, C. Paranthoen, J. Even, C. Labbé, H. Folliot, V. V. Moshchalkov, and S. Loualiche: *Phys. Rev. B* **74** (2006) 245315.
- 19) C. Paranthoen, N. Bertru, O. Dehaese, A. Le Corre, S. Loualiche, and B. Lambert: *Appl. Phys. Lett.* **78** (2001) 1751.
- 20) C. Cornet, C. Levallois, P. Caroff, H. Folliot, C. Labbé, J. Even, M. Hayne, and V. V. Moshchalkov: *Appl. Phys. Lett.* **87** (2005) 233111.
- 21) J. Ibanez, R. Cusco, S. Hernandez, L. Artus, M. Henini, A. Patane, L. Eaves, M. Roy, and P. A. Maksym: *J. Appl. Phys.* **99** (2006) 043501.
- 22) C. Cornet, A. Schliwa, J. Even, F. Doré, C. Celebi, A. Létoublon, E. Macé, C. Paranthoen, A. Simon, P. M. Koenraad, N. Bertru, D. Bimberg, and S. Loualiche: *Phys. Rev. B* **74** (2006) 035312.
- 23) F. Lelarge, B. Rousseau, D. Dagens, F. Poingt, F. Pommereau, and A. Accard: *IEEE Photonics Technol. Lett.* **17** (2005) 1369.
- 24) R. Schwertberger, D. Gold, and J. P. Reithmaier: *IEEE Photonics Technol. Lett.* **14** (2002) 735.
- 25) M. Sugawara, K. Mukai, Y. Nakata, H. Ishikawa, and A. Sakamoto: *Phys. Rev. B* **61** (2000) 7595.
- 26) P. Miska, C. Paranthoen, J. Even, N. Bertru, A. Le Corre, and O. Dehaese: *J. Phys.: Condens. Matter* **14** (2002) 12301.
- 27) A. E. Zhukov, A. R. Kovsh, N. A. Maleev, S. S. Mikhlin, V. M. Ustinov, A. F. Tsatsul'nikov, M. V. Maximov, B. V. Volovik, D. A. Bedarev, Yu. M. Shernyakov, P. S. Kop'ev, Zh. I. Alferov, N. N. Ledentsov, and D. Bimberg: *Appl. Phys. Lett.* **75** (1999) 1926.
- 28) C. Cornet, C. Labbé, H. Folliot, N. Bertru, O. Dehaese, J. Even, A. Le Corre, C. Paranthoen, C. Platz, and S. Loualiche: *Appl. Phys. Lett.* **85** (2004) 5685.